ChemComm

Hydrophilic 18F-labeled trans-5-oxocene (oxoTCO) for efficient construction of PET agents with improved tumor-to-background ratios in neurotensin receptor (NTR) imaging

Journal:	*ChemComm*
Manuscript ID	CC-COM-12-2018-009747.R1
Article Type:	Communication

ChemComm

COMMUNICATION

Hydrophilic ^{18}F-labeled *trans*-5-oxocene (oxoTCO) for efficient construction of PET agents with improved tumor-to-background ratios in neurotensin receptor (NTR) imaging

Received 00th January 20xx,
Accepted 00th January 20xx

DOI: 10.1039/x0xx00000x

www.rsc.org/

Mengzhe Wang[a, #], Raghu Vannam[b, #], William Lambert[b], Yixin Xie[b], Hui Wang[a], Ben Giglio[a], Xiaofen Ma[a], Zhanhong Wu[a], Joseph Fox[b]*, and Zibo Li[a]*

Described here is an ^{18}F-labeled *trans*-5-oxocene (oxoTCO) that through tetrazine ligation is used to construct a PET probe for neurotensin receptor (NTR) imaging. PET probe construction proceeds in 70% RCY based on ^{18}F-oxoTCO and is complete within seconds. The *in vivo* behaviour of oxoTCO based PET probe was compared with analogous probes that were prepared from ^{18}F-labeled s-TCO and d-TCO tracers. The hydrophilic ^{18}F-oxoTCO probe showed a significantly higher tumor-to-background ratio while displaying comparable tumor uptake relative to the ^{18}F-dTCO and ^{18}F-sTCO derived probes.

Bioorthogonal reactions are unnatural reactions that can proceed in biological context with minimal interference from biological functionality.[1-4] Tetrazine ligation—the inverse electron Diels-Alder reaction between s-tetrazines and alkenes—is a rapid biorthogonal reaction involving *trans*-cyclooctene (TCO), norbornene, cyclopropenes and α-olefins dienophiles.[5-9] The fast kinetics of the tetrazine ligation with TCO has enabled a range of biomedical applications, including applications in nuclear medicine.[10-13] We have shown that the rate of tetrazine ligation can be further accelerated through the use of conformationally strained *trans*-cyclooctene derivatives s-TCO and the more hydrophilic d-TCO with rates as fast as 3.3 x 10^6 $M^{-1}s^{-1}$ and 3.7 x 10^5 $M^{-1}s^{-1}$, respectively (Scheme 1A).[14, 15]

Positron emission tomography (PET) is a non-invasive imaging modality that allows non-invasive monitoring of diverse biological process in vivo. The most commonly used PET isotope, ^{18}F (half-life ~110 min), has become widely used for the attachment of radiolabels to biological macromolecules. In order to overcome the limitations imposed by short half-life and the low concentration of F-18, our labs have developed fast and

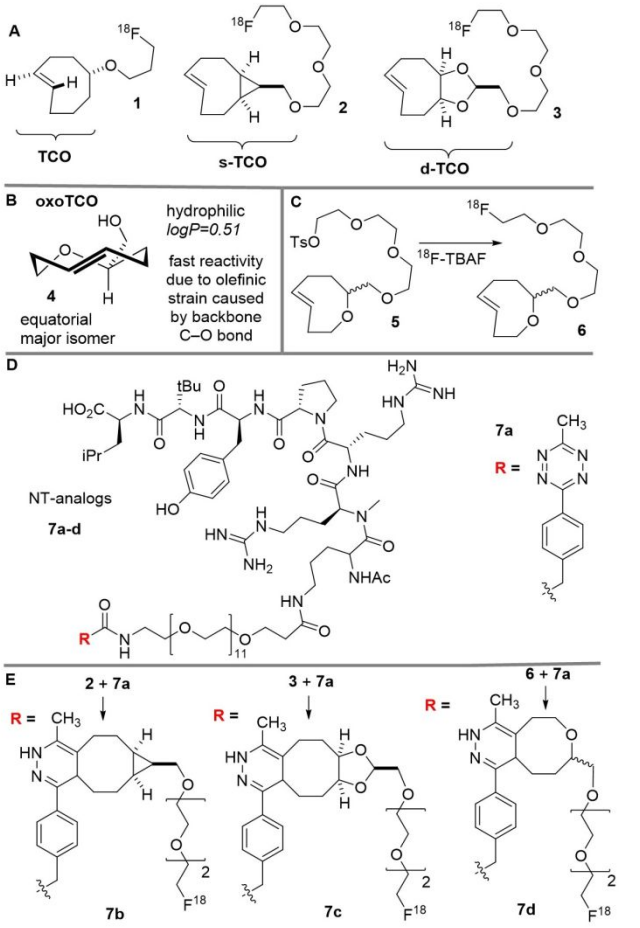

Scheme 1 (A) ^{18}F-labeled trans-cyclooctene radiotracers based on TCO, s-TCO and d-TCO. (B) The recently developed hetero-trans-cyclooctene oxoTCO displays fast reactivity and higher hydrophilicity due to the oxygen in the cyclic backbone. (C) Radio synthesis of ^{18}F-labeled oxoTCO. (D) An analog of neurotensin (NT) with a conjugated tetrazine (**7a**) is a precursor to ^{18}F-labeled analogs for cancer imaging. (E) ^{18}F-labeled NT analogs **7b-d** from s-TCO, d-TCO, and oxoTCO, respectively. Only one isomer is shown for the Diels-Alder adducts.

[a] *Department of Radiology and Biomedical Research Imaging Center, University of North Carolina at Chapel Hill, Chapel Hill, North Carolina 27599, USA*
Email: ziboli@med.unc.edu
[b] *Brown Laboratories, Department of Chemistry and Biochemistry, University of Delaware, Newark, Delaware 19716, USA*
Email: jmfox@udel.edu

Electronic Supplementary Information (ESI) available: [details of any supplementary information available should be included here]. See DOI: 10.1039/x0xx00000x

efficient labelling methods to generate ^{18}F-labeled PET probes with optimized lesion-to-background contrast.[16-19] In 2010, ^{18}F-labeled TCO **1** (Scheme 1A) was described and Diels-Alder conjugates were subsequently used in a range of imaging applications.[20] More recently, we introduced ^{18}F-labeled s-TCO **2** (Scheme 1A) as the most reactive dienophile for ^{18}F probe construction, and subsequently a similar design was used by Bormans and coworkers to prepare ^{18}F-labeled s-TCO and d-TCO probes.[21-23] While the ^{18}F-attachment using these strained TCO probes is very efficient, the acquired images can have relatively high background, leading to a modest target-to-background ratio. We hypothesized that the background is caused by the hydrophobicity of the probe, leading to high background signal from both renal and hepatic pathways.[24]

Several approaches have been explored to improve the physiochemical properties of tetrazine ligation reaction partners. Smaller dienophiles, including cyclopropenes and cyclobutenes, have been developed as lower molecular weight alternatives to *trans*-cyclooctenes, but with a compromise of reaction rate.[25, 26] ^{18}F-labeled dialkyl-*s*-tetrazines have also been developed to increase the hydrophilicity of Diels-Alder conjugates for PET imaging applications.[27] Recently, oxygen-containing TCO derivatives with improved solubility properties have been described.[28] A *trans*-5-oxocene (oxoTCO, **4**) was shown to display enhanced reactivity compared to 5-hydroxy-*trans*-cyclooctene, and enhanced hydrophilicity (logP 0.51) relative to 5-hydroxy-*trans*-cyclooctene (logP 1.11) and d-TCO (logP 0.91). Here, we describe the preparation of labelling precursor **5** and ^{18}F-labeled oxoTCO **6**, and compare the in vivo imaging results for a series of probes **7b-d** that target the neurotensin (NT) receptor, which is upregulated in prostate, pancreatic, lung, and colorectal cancer.[29-32] Probes **7b-d** were prepared by combining a tetrazine-peptide conjugate **7a** with ^{18}F-s-TCO (**2**), ^{18}F-d-TCO (**3**) and ^{18}F-oxoTCO (**6**). A significant improvement in tumor-to-background ratio was realized by using the oxoTCO-based probe **7d** in place of the more hydrophobic probes **7b** and **7c**.

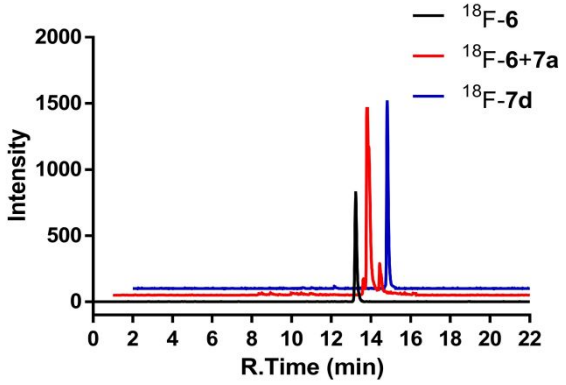

Figure 1 Radio-HPLC profile of freshly prepared (a) ^{18}F-**6** (b) crude reactions of ^{18}F-**6** and **7a** and freshly prepared (c) ^{18}F-**7d**.

Radiochemical synthesis were modeled after our previously described procedure for preparing ^{18}F-s-TCO **2**.[23] oxoTCO was prepared as a 3.4:1 mixture of equatorial:axial diastereomers as described previously.[28] The ^{18}F-labeling precursor **5** was prepared by treating diastereomers of oxoTCO (**4**) with triethylene glycol di(*p*-toluenesulfonate), followed by treatment with ^{18}F-TBAF to provide **6** in 15.2 ± 1.9% radiochemical yield. Efforts to improve the radiochemical yield of **6** by increasing the concentration of **5** or prolonging reaction time were unsuccessful. While the radiochemical yield for tosylate displacement was moderate, it is high enough to be useful and is in alignment with yields obtained in many procedures for F-18 probe construction.[33] Radiolabeled s-TCO and d-TCO were prepared in similar fashion, and cold standards were prepared using ^{19}F-TBAF. For ^{18}F-**6**, the radiochemical purity was >99% after initial purification (Figure 1). After incubation in 1 h in PBS, the radiochemical purity of **6** was 85.2%, indicating a level of stability that was good but not as high as a cold oxoTCO compound stored under similar conditions.[28] In a previous study, we found that oxoTCO decomposes more rapidly under conditions conducive to radical formation, and it may be that the radiolysis contributes to the decomposition of **6**. The oxoTCO derived probe **7d** was prepared by mixing **6** with **7a**. As shown in Figure 1b, there is only one major peak which aligns with ^{19}F-**7d**. No ^{18}F-**6** was left indicating a complete consumption of the ^{18}F labeled oxoTCO. The reactions to prepare **7b** and **7c** were similarly efficient, all three reactions can be completed in seconds with comparable conversion efficiency.

The logP values were evaluated for each of the ^{18}F-radiolabeled TCO tracers and their derived NT-probes. The logP for ^{18}F-oxoTCO **6** was 0.57 ± 0.02, which was lower than either ^{18}F-s-TCO **2** (logP 0.95 ± 0.02) or ^{18}F-d-TCO **3** (logP 0.91 ± 0.02). Similar to the

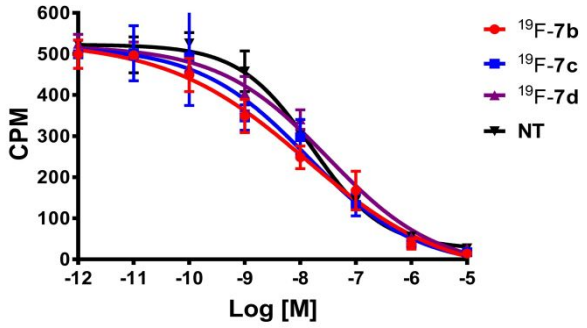

Figure 2 Competitive cell binding assays of **7b-d** and original NT peptide.

corresponding dienophiles, oxoTCO-derived probe **7d** is the most hydrophilic with logP of -2.47 ± 0.05, while s-TCO derived **7b** and d-TCO derived **7c** had logP values of -1.10 ± 0.04 and -1.59 ± 0.01, respectively.

The ^{19}F-labeled NT-probe compounds were subjected to *in vitro* competitive cell binding assay to ensure that the prosthetic linker does not compromise the binding affinity of the targeting moiety. As shown in Figure 2, ^{19}F-labeled probes **7b-d** showed comparable binding affinity with the unmodified NT peptide. The IC_{50} values for NT, and ^{19}F-labeled probes **7b**, **7c** and **7d** are 16.2 ± 2.7 nM, 20.5 ± 14.1 nM, 15.4 ± 3.4 nM and 31.6 ± 7.1 nM respectively.

We evaluated the *in vivo* behavior and targeting efficiency of all three PET tracers. 3.7 MBq (100µCi) doses of **7b-d** were injected into NTR positive PC-3 tumor-bearing mice. Static PET/CT scans were acquired at 0.5 and 3.5 hours post injection and the images are shown in Figure 3. As can be seen, tumors were clearly visualized in all the groups at both time points

indicating that all tracers have reasonable targeting efficiency *in vivo*. d-TCO derived tracer **7c** showed the highest tumor uptake of 2.1 ± 1.0 %ID/g at 0.5h post injection. Slightly lower uptake was observed for oxoTCO derived **7d** (1.7 ± 0.1 %ID/g) and s-TCO derived **7b** (1.5 ± 0.1% ID/g). Though d-TCO derived tracer **7c** showed higher uptake than the others, there is no significant difference between any two groups. At 3.5h post injection, the tumor uptakes in all three groups decreased significantly and showed comparable values around 1.1% ID/g.

Figure **3** shows the representative PET/CT images of PC-3 tumor-bearing mice after injecting probes **7b-d** and the corresponding tumor to liver and tumor to muscle ratios. Although ^{18}F-d-TCO derived **7c** showed the highest tumor uptake among the three tracers, it also showed relatively high

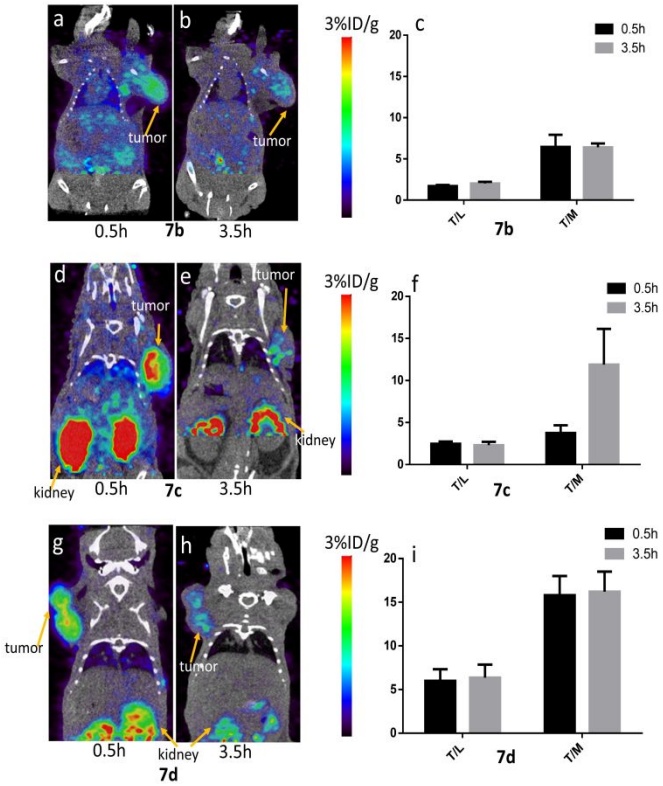

Figure 3 Tumor-to-background is improved by using oxo-TCO derived **7d**. Representative PET/CT images of PC-3 tumor-bearing mice at 0.5h and 3.5h post-injection of (a)(b) **7b**, (d)(e) **7c** and (g)(h) **7d**. Tumor to liver and tumor to muscle ratio of (c) **7b**, (f) **7c** and (i) **7d** in mice bearing PC-3 xenografts at 0.5 and 3.5h post-injection

background. High background was also observed with **7b**. The more hydrophilic ^{18}F-oxoTCO derived probe **7d** gave highest tumor-to-liver ratio and best tumor-to-muscle ratio of the three probes. As shown in Table 1, at 0.5 h post injection the tumor-to-muscle ratio was 6.5 ± 1.5 and 3.8 ± 0.9 for **7b** and **7c**, while the more hydrophilic **7d** showed a greatly improved tumor-to-muscle ratio of 15.8 ± 2.2. Given that the tumor uptake of **7d** is not the highest among the three compounds, it can be concluded that the high tumor-to-background ratio is due to low uptake in the muscle and liver. At 3.5h post injection, the high tumor-to-muscle ratio of **7d** was maintained at 16.2 ± 2.3, indicating a faster clearance rate at non-specific binding regions than at tumor sites. The tumor to muscle ratio of **7b** remained at 6.4 ± 0.5, whereas **7c** increased to 11.9 ± 4.3%, an effect that is possibly related to the reduced lipophilicity of dTCO-derived probe relative to the sTCO-derived probe. As expected, in all images the kidneys had the highest uptake for all PET agents, which could be attributed to the relativity small size and hydrophilicity of the three probes.

Table 1 Tumor to muscle uptake ratio of MePhTz-NT with different TCOs in PC-3 xenograft at 0.5 and 3.5h post-injection

Tumor/Muscle	0.5h	3.5h
7b	6.5 ± 1.5	6.4 ± 0.5
7c	3.8 ± 0.9	11.9 ± 4.3
7d	15.8 ± 2.2	16.2 ± 2.3

The targeting specificity of the **7d** was further confirmed by a blocking experiment in which 100 μg of NT peptide was coinjected with **7d** into PC-3 tumor-bearing mice and imaged at 0.5h post injection (Figure 4). The tumor uptake significantly decreased in the blocking group from 1.7 ± 0.1%ID/g to 0.8 ± 0.1%ID/g (P<0.05).

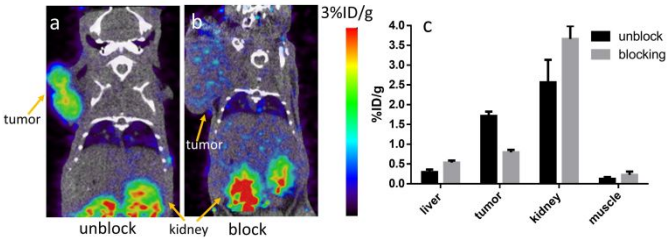

Figure 4 Representative PET/CT images of PC-3 tumor-bearing mice at 0.5h post-injection of **7d** (a) without and (b) with blocking dose. (c) Quantitative uptakes of major organs derived from PET images

In summary, an ^{18}F-labeled *trans*-5-oxocene (^{18}F-oxoTCO, **6**) for the rapid construction of PET probes via tetrazine ligation is described. The tracer showed comparable tumor uptake with the previously described s-TCO and d-TCO based method. However, the increased hydrophilicity from the oxoTCO enabled a faster clearance rate of the tracer from non-targeting organs, which lead to significantly higher tumor to background ratio compared with s-TCO and d-TCO counterparts. This newly developed 18F-oxoTCO dienophiles holds the great potential for PET probe construction for *in vivo* applications.

This work was supported by NIBIB (5R01EB014354-03), P30-CA016086-35-37 from the National Cancer Institute, and UNC Radiology Department and BRIC. Spectra were obtained with instrumentation supported by NIH grants P20GM104316, P30GM110758, S10RR026962, S10OD016267, 1S10OD023611 and NSF grants CHE-0840401, CHE-1229234.

Conflicts of interest

There are no conflicts to declare.

References

1. K. Lang and J. W. Chin, *ACS Chem Biol*, 2014, **9**, 16-20.
2. J. P. Meyer, P. Adumeau, J. S. Lewis and B. M. Zeglis, *Bioconjug Chem*, 2016, **27**, 2791-2807.
3. D. M. Patterson, L. A. Nazarova and J. A. Prescher, *ACS Chem Biol*, 2014, **9**, 592-605.
4. C. P. Ramil and Q. Lin, *Chem Commun (Camb)*, 2013, **49**, 11007-11022.
5. M. L. Blackman, M. Royzen and J. M. Fox, *J Am Chem Soc*, 2008, **130**, 13518-13519.
6. N. K. Devaraj, R. Weissleder and S. A. Hilderbrand, *Bioconjug Chem*, 2008, **19**, 2297-2299.
7. Y. J. Lee, Y. Kurra, Y. Yang, J. Torres-Kolbus, A. Deiters and W. R. Liu, *Chem Commun (Camb)*, 2014, **50**, 13085-13088.
8. A. Niederwieser, A. K. Spate, L. D. Nguyen, C. Jungst, W. Reutter and V. Wittmann, *Angew Chem Int Ed Engl*, 2013, **52**, 4265-4268.
9. B. L. Oliveira, Z. Guo, O. Boutureira, A. Guerreiro, G. Jimenez-Oses and G. J. Bernardes, *Angew Chem Int Ed Engl*, 2016, **55**, 14683-14687.
10. N. K. Devaraj, R. Upadhyay, J. B. Haun, S. A. Hilderbrand and R. Weissleder, *Angew Chem Int Ed Engl*, 2009, **48**, 7013-7016.
11. T. Reiner and B. M. Zeglis, *J Labelled Comp Radiopharm*, 2014, **57**, 285-290.
12. R. Rossin, T. Läppchen, S. M. van den Bosch, R. Laforest and M. S. Robillard, *Journal of Nuclear Medicine*, 2013, **54**, 1989-1995.
13. B. M. Zeglis, K. K. Sevak, T. Reiner, P. Mohindra, S. D. Carlin, P. Zanzonico, R. Weissleder and J. S. Lewis, *J Nucl Med*, 2013, **54**, 1389-1396.
14. A. Darko, S. Wallace, O. Dmitrenko, M. M. Machovina, R. A. Mehl, J. W. Chin and J. M. Fox, *Chem Sci*, 2014, **5**, 3770-3776.
15. M. T. Taylor, M. L. Blackman, O. Dmitrenko and J. M. Fox, *J Am Chem Soc*, 2011, **133**, 9646-9649.
16. B. C. Giglio, H. Fei, M. Wang, H. Wang, L. He, H. Feng, Z. Wu, H. Lu and Z. Li, *Theranostics*, 2017, **7**, 1524-1530.
17. Z. Wu, L. Li, S. Liu, F. Yakushijin, K. Yakushijin, D. Horne, P. S. Conti, Z. Li, F. Kandeel and J. E. Shively, *Journal of Nuclear Medicine*, 2014, **55**, 1178-1184.
18. Z. Wu, S. Liu, M. Hassink, I. Nair, R. Park, L. Li, I. Todorov, J. M. Fox, Z. Li, J. E. Shively, P. S. Conti and F. Kandeel, *J Nucl Med*, 2013, **54**, 244-251.
19. M. Wang, C. Mao, H. Wang, X. Ling, Z. Wu, Z. Li and X. Ming, *Mol Pharm*, 2017, **14**, 3391-3398.
20. Z. Li, H. Cai, M. Hassink, M. L. Blackman, R. C. Brown, P. S. Conti and J. M. Fox, *Chem Commun (Camb)*, 2010, **46**, 8043-8045.
21. E. M. F. Billaud, S. Belderbos, F. Cleeren, W. Maes, M. Van de Wouwer, M. Koole, A. Verbruggen, U. Himmelreich, N. Geukens and G. Bormans, *Bioconjug Chem*, 2017, **28**, 2915-2920.
22. E. M. F. Billaud, E. Shahbazali, M. Ahamed, F. Cleeren, T. Noel, M. Koole, A. Verbruggen, V. Hessel and G. Bormans, *Chem Sci*, 2017, **8**, 1251-1258.
23. M. Wang, D. Svatunek, K. Rohlfing, Y. Liu, H. Wang, B. Giglio, H. Yuan, Z. Wu, Z. Li and J. Fox, *Theranostics*, 2016, **6**, 887-895.
24. E. Kozma, I. Nikic, B. R. Varga, I. V. Aramburu, J. H. Kang, O. T. Fackler, E. A. Lemke and P. Kele, *Chembiochem*, 2016, **17**, 1518-1524.
25. J. Yang, J. Seckute, C. M. Cole and N. K. Devaraj, *Angew Chem Int Ed Engl*, 2012, **51**, 7476-7479.
26. K. Liu, B. Enns, B. Evans, N. Wang, X. Shang, W. Sittiwong, P. H. Dussault and J. Guo, *Chem Commun (Camb)*, 2017, **53**, 10604-10607.
27. C. Denk, D. Svatunek, T. Filip, T. Wanek, D. Lumpi, J. Frohlich, C. Kuntner and H. Mikula, *Angew Chem Int Ed Engl*, 2014, **53**, 9655-9659.
28. W. D. Lambert, S. L. Scinto, O. Dmitrenko, S. J. Boyd, R. Magboo, R. A. Mehl, J. W. Chin, J. M. Fox and S. Wallace, *Org Biomol Chem*, 2017, **15**, 6640-6644.
29. C. Morgat, A. K. Mishra, R. Varshney, M. Allard, P. Fernandez and E. Hindie, *J Nucl Med*, 2014, **55**, 1650-1657.
30. N. C. Valerie, E. V. Casarez, J. O. Dasilva, M. E. Dunlap-Brown, S. J. Parsons, G. P. Amorino and J. Dziegielewski, *Cancer Res*, 2011, **71**, 6817-6826.
31. F. Souaze, S. Dupouy, V. Viardot-Foucault, E. Bruyneel, S. Attoub, C. Gespach, A. Gompel and P. Forgez, *Cancer Res*, 2006, **66**, 6243-6249.
32. M. Alifano, F. Souaze, S. Dupouy, S. Camilleri-Broet, M. Younes, S. M. Ahmed-Zaid, T. Takahashi, A. Cancellieri, S. Damiani, M. Boaron, P. Broet, L. D. Miller, C. Gespach, J. F. Regnard and P. Forgez, *Clin Cancer Res*, 2010, **16**, 4401-4410.
33. O. Jacobson, D. O. Kiesewetter and X. Chen, *Bioconjugate Chemistry*, 2015, **26**, 1-18.